β-catenin inhibition disrupts the homeostasis of osteogenic/adipogenic differentiation leading to the development of glucocorticoid-induced osteonecrosis of femoral head

Chenjie Xia[1,2*], Huihui Xu[1*], Liang Fang[1], Jiali Chen[1], Wenhua Yuan[1], Danqing Fu[3], Xucheng Wang[1], Bangjian He[4], Luwei Xiao[1], Chengliang Wu[1], Peijian Tong[4], Di Chen[5†], Pinger Wang[1†], Hongting Jin[1†]

[1] Institute of Orthopadics and Traumatology, The First Affiliated Hospital of Zhejiang Chinese Medical University, Hangzhou, Zhejiang 310053, China
[2] Department of Orthopedic Surgery, Lihuili Hospital Affiliated to Ningbo University, Ningbo, Zhejiang 315041, China
[3] School of Basic Medical Sciences, Zhejiang Chinese Medical University, Hangzhou, Zhejiang 310053, China
[4] Department of Orthopedic Surgery, the First Affiliated Hospital of Zhejiang Chinese Medical University, Hangzhou, Zhejiang 310003, China
[5] Faculty of Pharmaceutical Sciences, Shenzhen Institutes of Advanced Technology, Chinese Academy of Sciences, Shenzhen 518055, China

*These authors have an equal contribution to this work.
[†]Corresponding author:
Di Chen
Faculty of Pharmaceutical Sciences
Shenzhen Institute of Advanced Technology
Chinese Academy of Sciences
1068, Xueyuan Road
Shenzhen 518055, China
Email: di.chen@siat.ac.cn

Ping-er Wang
Institute of Orthopaedics and Traumatology
The First Affiliated Hospital of Zhejiang Chinese Medical University
548, Binwen Road
Hangzhou, Zhejiang Province 310053, China
Email: pingerwang@zcmu.edu.cn

Hongting Jin
Institute of Orthopaedics and Traumatology
The First Affiliated Hospital of Zhejiang Chinese Medical University
548, Binwen Road
Hangzhou, Zhejiang Province 310053, China.
Email: hongtingjin@zcmu.edu.cn

Abstract

Glucocorticoid-induced osteonecrosis of the femoral head (GONFH) is a common refractory joint disease characterized by bone damage and the collapse of femoral head structure. However, the exact pathological mechanisms of GONFH remain unknown. Here, we observed abnormal osteogenesis and adipogenesis associated with decreased β-catenin in the necrotic femoral head of GONFH patients. In vivo and in vitro studies further revealed that glucocorticoid exposure disrupted osteogenic/adipogenic differentiation bone marrow stromal cells (BMSCs) by inhibiting β-catenin signaling in glucocorticoid-induced GONFH rats. $Col2^+$ lineage largely contributes to BMSCs, and was found an osteogenic commitment in the femoral head through 9 months of lineage trace. Specific deletion of *β-catenin* in $Col2^+$ cells shifted their commitment from osteoblasts to adipocytes, leading to a full spectrum of disease phenotype of GONFH in adult mice. Overall, we uncover that β-catenin inhibition disrupting the homeostasis of osteogenic/adipogenic differentiation contribute to the development of GONFH, and identify an ideal genetic modified mouse model of GONFH.

Keywords: Glucocorticoid; Osteonecrosis of the femoral head; β-catenin; Osteogenic/adipogenic differentiation; $Col2^+$ lineage

Introduction

Glucocorticoids, potent immunity regulators, are widely used in the treatment of various autoimmune diseases such as systemic lupus erythematosus (SLE), nephrotic syndrome (NS) and rheumatoid arthritis (RA)*(Yang et al., 2021)*. However, excessive usage of glucocorticoids has been reported to cause severe adverse effects, especially femoral head osteonecrosis in the joint*(Zaidi et al., 2010; Tao et al., 2017)*. As a destructive joint disease, glucocorticoid-induced osteonecrosis of the femoral head (GONFH) disables about 100,000 Chinese and more than 20,000 Americans annually*(Petek et al., 2019; Zhao et al., 2020)*, bringing a huge financial burden on the society. Currently, there is no ideal medical treatment for GONFH due to its unclear pathological mechanisms. Most patients eventually have to undergo a joint replacement surgery*(Scaglione et al., 2015)*. Therefore, in-depth study of GONFH pathogenesis is urgently needed.

Previous *ex-vivo* studies on human necrotic femoral heads revealed prominent pathological features of GONFH including fat droplet clusters, trabecular bone loss, empty lacunae of osteocyte at the early stage and extra subchondral bone destruction, structure collapse at the late stage*(Qin et al., 2015; Wang et al., 2018a)*. Glucocorticoid-induced animal models are commonly used to study GONFH pathogenesis, which mimic the early necrotic changes of GONFH but without structure collapse*(Zheng et al., 2018)*. Several hypotheses, such as damaged blood supply*(Sun et al., 2021; Wang et al., 2018b)*, abnormal lipid metabolism*(Lavernia et al., 1999; Chang et al., 1993)* and bone cell apoptosis*(Chen et al., 2022; Zalavras et al., 2003)* have been proposed to explain the occurrence and development of GONFH. However, the therapies developed according to the guideline established based on these theories have not been successful in prevention of GONFH progression. Clinical evidence about decreased replication and osteogenic differentiation capacity of bone marrow mesenchymal stromal cells (BMSCs)*(Lee et al., 2006; Wang et al., 2008; Houdek et al., 2016)* and the efficacy of BMSCs transplantation*(Wang et al., 2019a; Tabatabaee et al., 2015; Gangji and Hauzeur, 2005)* in GONFH patients indicate that GONFH might be a BMSCs-related disease. BMSCs contain mesenchymal progenitor cells which give rise to osteoblasts and adipocytes, and glucocorticoids have been shown to regulate osteogenic/adipogenic differentiation of BMSCs *in vitro*(*Yin et al., 2006; Han et al., 2019)*. Various treatments targeting on promoting osteogenic differentiation of BMSCs alleviate early necrotic phenotype in glucocorticoid-induced GONFH animal models*(Chen et al., 2020; Zhu et al., 2020; Feng et al., 2022)*. Thus, we hypothesize that imbalanced osteogenic/adipogenic differentiation of BMSCs plays a dominant role in GONFH pathogenesis. Recent lineage tracing and single-cell RNA sequencing studies revealed that BMSCs are a group of heterogeneous multipotent cells*(Gao et al., 2021)*, and skeletal-derived mesenchymal progenitor cells including collagen II $(Col2)^+$ lineage and Osterix $(Osx)^+$ lineage compose a large proportion of BMSCs*(Ono et al., 2014; Liu et al., 2013)*. However, which sub-population of BMSCs significantly contributes to the GONFH pathogenesis remains unknown.

BMSCs differentiation is a complex process and is regulated by multiple signaling pathways. Among them, canonical Wnt/β-catenin signaling functions as a switch in determining osteogenic/adipogenic differentiation of BMSCs*(Song et al., 2012)*. When β-catenin is

accumulated in the nucleus, interacting with TCF/Lef transcription factors to activate downstream target genes including Runt-related transcription factor 2 (Runx2) and Osterix*(Yuan et al., 2016)*. On the contrary, inhibition of β-catenin induces expressions of CCAAT/enhancer binding protein alpha (C/EBPα) and peroxisome proliferator activated receptor gamma (PPAR-γ) for adipogenesis*(Takada et al., 2009; Xu et al., 2016)*. Our previous study showed a significant decrease of β-catenin in the glucocorticoid-induced GONFH rat model*(Zhang et al., 2019)*. Other groups also reported an involvement of β-catenin signaling in GONFH development*(Zhang et al., 2021; Chen et al., 2019; Zhao et al., 2021; Yu et al., 2016; Zhang et al., 2015)*.

Here, abnormal osteogenesis and adipogenesis with decreased β-catenin signaling were observed in the necrotic femoral heads of GONFH patients and glucocorticoid-induced GONFH rats. Activation of β-catenin signaling effectively alleviated the necrotic changes in GONFH rats by restoring glucocorticoid exposure-induced imbalanced osteogenic/adipogenic differentiation of BMSCs. Interestingly, specific deletion of *β-catenin* in $Col2^{+}$ cells, but not Osx^{+} cells led to a full spectrum of disease phenotype of GONFH in mice even including subchondral bone destruction and femoral head collapse. Our present study provided novel molecular mechanisms of GONFH pathogenesis, and an ideal genetic modified mouse model for GONFH study.

Results

Abnormal osteogenesis and adipogenesis with decreased β-catenin in necrotic femoral head of GONFH patients

To determine the pathogenesis of GONFH, we harvested the surgical specimens from GONFH patients with femoral head necrosis (n=15) and samples from trauma patients without femoral head necrosis (n=10). Compared to the non-necrotic femoral head, we observed subchondral bone destruction (Figure 1A, black asterisk), liquefied necrotic foci (Figure 1A, black arrow), deformed and collapsed outline in the necrotic femoral head. μCT analysis further showed sparse and cracked trabeculae in the collapsed region (Figure 1B, red box) and liquefied necrotic region (Figure 1B, yellow box) compared to the corresponding regions (Figure 1B, white boxes) in the non-necrotic femoral heads, which were further confirmed by the decreased BV/TV, Tb.N and Tb.Th and increased Tb.Sp (Figure 1C). The representative images of ABH staining (Figure 1D) revealed sparse trabeculae, massive accumulated fat droplets (Figure 1D, black triangles), numerous empty lacunae of osteocytes (Figure 1D, black arrows) and extensive subchondral bone

destruction (Figure 1D, yellow arrows) in the necrotic femoral head. Histomorphological quantitative analyses showed decreased trabecular bone area (Figure 1E), increased fat droplet area (Figure 1E) and empty lacunae rate (Figure 1F) in the necrotic femoral heads. TUNEL staining revealed more apoptotic osteocytes in the necrotic femoral head (Figure 1G). We then detected the expression of osteogenic (Runx2, Osterix) and adipogenic (FABP4, PPAR-γ, CEBP/α) marker genes. The results of IHC staining showed a down-regulation of Runx2 and an up-regulation of FABP4 in the necrotic regions (Figure 1H). Western blot analysis showed increased expressions of PPAR-γ and CEBP/α and a decreased expression of Osterix in the human necrotic femoral head tissues (Figure 1I). These findings indicate an involvement of abnormal osteogenesis and adipogenesis during GONFH pathogenesis. β-catenin can regulate osteogenesis and adipogenesis downstream target genes (Runx2, Osterix, FABP4, PPAR-γ and CEBP/α) expressions*(Tencerova and Kassem, 2016)*. The significant decrease of β-catenin in the necrotic femoral heads (Figure 1G, 1H) indicate an important role of β-catenin signaling in GONFH pathogenesis.

Inhibition of β-catenin signialing leads to abnormal osteogenesis and adipogenesis in glucocorticoid-induced GONFH rats

To further analyze the role of β-catenin in GONFH pathogenesis, a glucocorticoid-induced GONFH rat model was established by continuous MPS induction, as previously described*(Zheng et al., 2018)*. Gross anatomy analysis showed a local melanocratic region on the femoral head surface of GONFH rats without any structure deformity or collapse (Figure 2A, black arrow). No color change was observed on the femoral head surface from the Wnt agonist 1 treated rats. μCT images and quantitative analysis of bone microstructure showed severe trabecular bone loss in the femoral head of GONFH rats, especially in the subchondral region (Figure 2A, 2B). Systemic injection of Wnt agonist 1 effectively increased bone mass (Figure 2A), and alleviated decreased BV/TV, Tb.N and Tb.Th and increased Tb.Sp in GONFH rats (Figure 2B). ABH staining and histomorphological quantitative analysis revealed that the GONFH rats presented sparse trabeculae, massive fat accumulation (Figure 2C, black arrow) and numerous empty lacunae of osteocytes (Figure 2C, black arrows) in the necrotic region of femoral heads (Figure 2C-2E). However, no subchondral bone destruction, femoral head collapse and deformity was occurred in this GONFH rat model (Figure 2C). TUNEL staining reveled increased apoptotic osteocytes in the

119 femoral heads of GONFH rats (Figure 2F). ALP is an osteoblast marker reflecting the capacity of
120 osteogenesis. FABP4 is essential for lipid formation and metabolism. The decreased β-catenin and
121 ALP expressions and increased FABP4 expression confirmed abnormal osteogenesis and
122 adipogenesis during rat GONFH development (Figure 2G, 2H), consistent with the findings in
123 human GONFH femoral heads. Interestingly, activation of β-catenin by systematically injecting
124 Wnt agonist 1 for 6 weeks attenuated the early necrotic changes (Figure 2C-2E) and osteocyte
125 apoptosis (Figure 2F), and restored ALP and FABP4 expressions in the femoral head of GONFH
126 rats (Figure 2G, 2H). Overall, these data indicate that β-catenin inhibition-induced abnormal
127 osteogenesis and adipogenesis contributes to GONFH pathogenesis.

128 **β-catenin directs dexamethasone-induced osteogenic/adipogenic differentiation of rat**
129 **BMSCs**

130 We further investigated cellular mechanisms involved in the necrotic femeral head of
131 glucocorticoid-induced GONFH rats. Primary bone marrow cells were extracted from the
132 proximal femur of 4-week-old SD rats and cultivated to P3. Flow cytometry analysis identified
133 that they were BMSCs, with $CD90^+$, $CD29^+$, $CD45^-$ and $CD11b^-$ characteristics (Figure 3A). ALP
134 staining showed that the osteogenic differentiation of BMSCs were significantly inhibited after
135 exposing to 10^2 nM or higher concentration of Dex for 7 days (Figure 3B). Oil red O staining
136 showed a progressive adipogenic differentiation of BMSCs with the increased concentration of
137 Dex (Figure 3B). These findings indicated that increased adipogenic differentiation and decreased
138 osteogenic differentiation of BMSCs caused the abnormal osteogenesis and adipogenesis, finally
139 leading to the femoral head necrosis in GONFH rats. The decreased expressions of β-catenin,
140 Runx2, ALP and increased expressions of PPAR-γ, CEBP/α further revealed that Dex exposure
141 inhibited β-catenin signaling, and redirected BMSC differentiation from osteoblasts to adipocytes
142 (Figure 3C, 3D). However, this Dex-induced abnormal differentiation of BMSCs were restored by
143 SKL2001 through activation of β-catenin singling (Figure 3E-3G). Taking together, these findings
144 suggest that β-catenin inhibition redirects the direction of BMSC differentiation, contributing to
145 the GONFH development.

146 **Loss-of-function of β-catenin in $Col2^+$, but not Osx^+, -expressing cells leads to a GONFH-like**
147 **phenotype in femoral head**

148 Skeletal progenitor cells is a major source of BMSCs, and both $Col2^+$ lineage and Osx^+

149 lineage can trans-differentiate into BMSCs*(Gao et al., 2021; Ono et al., 2014)*. To determine
150 which subset of BMSCs contributes more to GONFH pathogenesis, we generated *β-catenin*^{Col2ER}
151 mice and *β-catenin*^{OsxER} mice, in which *β-catenin* gene was specifically deleted in Col2^{+} cells and
152 Osx^{+} cells, respectively. For mapping their cell fate in the femoral head, we induced *Tomato*^{Col2ER}
153 mice and *Tomato*^{OsxER} mice at 2-weeks old and analyzed at the age of 1 month. The fluorescent
154 images showed that Col2^{+} cells were evidently expressed in the chondrocytes of articular cartilage,
155 secondary ossification center and growth plate (Figure 4A, white arrowheads), osteoblasts (Figure
156 4A, green arrowheads), osteocytes (Figure 4A, yellow arrowheads) and stromal cells (Figure 4A,
157 red arrowheads) underneath the growth plate, while Osx^{+} cells were identified only in osteoblasts,
158 osteocytes and stromal cells underneath the growth plate (Figure 4A). We then trace Col2^{+} lineage
159 for 9 months and found that Col2^{+} chondrocytes in secondary ossification center and growth plate
160 were replaced by Col2^{+} osteoblasts, osteocytes and stromal cells with age (Figure 4B), and these
161 Col2^{+} cells continuously produced osteoblasts and osteocytes in the femoral head (Figure 4B).
162 These findings indicated the self-renew ability and osteogenic commitment of Col2^{+} cells. We also
163 induced *Tomato*^{Col2ER} mice at the age of 1 month, but identified a poor *Cre*-recombinase efficiency
164 24 hours and 3 months later (Figure 4C). IHC assay showed a significant decrease of β-catenin in
165 the femoral head of 3-month-old *β-catenin*^{Col2ER} mice and *β-catenin*^{OsxER} mice (Figure 4D, 4E),
166 indicating successful establishments of these *β-catenin* conditional knockout mouse models.

167 Then, we analyzed morphologic changes of the femoral head from 3-months old
168 *β-catenin*^{Col2ER} mice and *β-catenin*^{OsxER} mice. No change of appearance was observed on the
169 femoral head both in *β-catenin*^{Col2ER} mice and *β-catenin*^{OsxER} mice compared to *Cre*-negative
170 littermates (Figure 5A, 6A). μCT images and quantitative analysis of decreased BV/TV, Tb.N,
171 Tb.Th and increased Tb.Sp indicated that both *β-catenin*^{Col2ER} mice and *β-catenin*^{OsxER} mice
172 presented severe bone loss in the femoral heads (Figure 5B, 6B). ABH staining and
173 histomorphological analysis further revealed that bone trabeculae were extensively replaced by fat
174 droplet clusters in the femoral head (especially in the subchondral region) of *β-catenin*^{Col2ER} mice
175 (Figure 5C, 5D), similar to the necrotic femoral heads in GONFH patients and
176 glucocorticoid-induced rat models. However, no fat droplet accumulation but only sparse and thin
177 bone trabeculae were observed in the femoral head of *β-catenin*^{OsxER} mice (Figure 6C, 6D).
178 Compared to *Cre*-negative littermates, the number of empty lacunae was increased in the femoral

179 head in *β-catenin*^{Col2ER} mice (Figure 5E), but no changed in *β-catenin*^{OsxER} mice (Figure 6E).
180 TUNEL staining reveled more apoptotic osteocytes in *β-catenin*^{Col2ER} mice compared to
181 *Cre*-negative littermates (Figure 5F). All these findings indicate that loss-of-function of β-catenin
182 in Col2^{+} cells, but not in Osx^{+} cells, led to an GONFH-like phenotype in femoral head.
183 Furthermore, decreased Runx2, ALP and increased PPAR-γ, CEBP/α expressions in
184 *β-catenin*^{Col2ER} mice (Figure 5G) revealed that this GONFH-like phenotype was caused by
185 imbalance of osteogenic/adipogenic differentiation of Col2^{+} cells.

186 **Older *β-catenin*^{Col2ER} mice display subchondral bone destruction and collapse tendency in**
187 **the femoral heads**

188 Femoral head collapse occurs at the end-stage of GONFH and represents a poor joint
189 function*(Hines et al., 2021)*. To determine the occurrence of femoral head collapse, we further
190 analyzed 6-month-old *β-catenin*^{Col2ER} mice. Gross appearance showed that older *β-catenin*^{Col2ER}
191 mice lost smooth and regular outline on the femoral heads compared to *Cre*-negative littermates
192 and 3-month-old *β-catenin*^{Col2ER} mice (Figure 7A). μCT images showed severe bone loss (Figure
193 7B, 7C), subchondral bone destruction (Figure 7B, yellow arrows), local collapse (Figure 7B, red
194 arrows) and integral deformity (Figure 7B, red dotted lines) in the femoral heads of older
195 *β-catenin*^{Col2ER} mice. μCT quantitative analysis confirmed a significant increase of subchondral
196 bone defect area on the femoral head surface in older *β-catenin*^{Col2ER} mice (Figure 7D). Besides of
197 these early necrotic changes including sparse bone trabeculae, accumulated fat droplets (Figure 7E,
198 black triangles) and increased empty lacunae of osteoctye (Figure 7E, black arrows, Figure 7F),
199 ABH staining also showed subchondral bone destruction (Figure 7E, yellow arrows), femoral head
200 collapse or deformity (Figure 7E, red arrows and red dotted lines) in older *β-catenin*^{Col2ER} mice.
201 Compared to *Cre*-negative littermates, the older *β-catenin*^{Col2ER} mice presented a decrease of
202 loading-bearing stiffness, indicating a poor biomechanical support of the femoral heads (Figure
203 7G).

204 **Wnt agonist 1 could not alleviate GONFH-like phenotype in *β-catenin*^{Col2ER} mice**

205 As the therapeutic effects of Wnt agonist 1 on rat GONFH, we further determined whether it
206 could alleviate the GONFH-like phenotype in *β-catenin*^{Col2ER} mice. After induction with TM,
207 *β-catenin*^{Col2ER} mice were immediately injected with Wnt agonist 1 three times once week until
208 they were analyzed at the age of 3 months. However, μCT images and quantitative analysis of

209 BV/TV, Tb.N, Tb.Th and Tb.Sp showed severe bone loss were not restored in *β-catenin*^{Col2ER} mice
210 by treating with Wnt agonist 1 (Figure 8A, 8B). Accumulated fat droplets, sparse trabeculae and
211 empty lacunae were still existed in the femoral heads of Wnt agonist 1 treated *β-catenin*^{Col2ER} mice
212 (Figure 8C-8E). IHC staining showed no change of decreased ALP and increased FABP4 in the
213 femoral heads of *β-catenin*^{Col2ER} mice after Wnt agonist 1 treatment (Figure 8F, 8G). These
214 findings indicate that Wnt agonist 1 could not restore the imbalanced osteogenic/adipogenic
215 differentiation of Col2^{+} cells in *β-catenin*^{Col2ER} mice.

216 **Discussion**

217 Despite it is well known that glucocorticoids are the certain etiology of GONFH, its
218 pathogenesis remains largely unknown. Current evidence including reduced osteogenic
219 differentiation ability of BMSCs from GONFH patients and clinical therapeutical effects of
220 BMSCs transplantation indicates that GONFH could be resulted from abnormal differentiation of
221 BMSCs*(Houdek et al., 2016; Wang et al., 2019a; Tabatabaee et al., 2015; Gangji and Hauzeur,*
222 *2005)*. Glucocorticoid-induced animal models are commonly used for GONFH research, and
223 several previous studies have revealed that direct BMSCs modifications with miRNA*(Cao et al.,*
224 *2021; Gu et al., 2016)*, lncRNA*(Wang et al., 2018c; Xu et al., 2022)* and circRNA*(Chen et al.,*
225 *2020; Xiang et al., 2020)* or microenvironment interventions by injecting platelet-rich plasma*(Xu*
226 *et al., 2021; Wang et al., 2022)*, exosome*(Li et al., 2020; Fang et al., 2019)* and growth
227 factors*(Guzman et al., 2021; Rackwitz et al., 2012)* could promote osteogenic differentiation of
228 BMSCs and exhibit anti-GONFH effects in animals. In the present studies, we found severe
229 trabecular bone loss and massive fat droplets accumulation in the necrotic femoral heads of
230 GONFH patients and glucocorticoid-induced GONFH rats, confirming increased adipogenesis and
231 decreased osteogenesis in GONFH pathogenesis. Dex inhibited osteogenic differentiation of rat
232 BMSCs and promoted their adipogenic differentiation, revealing that this abnormal osteogenesis
233 and adipogenesis in GONFH rats were caused by the imbalance in osteogenic/adipogenic
234 differentiation of BMSCs. As β-catenin plays an important role in BMSCs differentiation, we then
235 analyzed its role in GONFH pathogenesis. The results showed a significant inhibition of β-catenin
236 signaling in the necrotic femoral heads of GONFH patients and glucocorticoid-induced GONFH
237 rats, while Wnt agonist 1 attenuated accumulated fat droplets and sparse trabeculae in GONFH
238 rats by activation of β-catenin signaling. The subsequent cellular experiments revealed that

239 β-catenin activation restored the imbalance of osteogenic/adipogenic differentiation of BMSCs
240 caused by long-term exposure of Dex. Overall, these findings indicate that β-catenin
241 inhibition-induced imbalanced osteogenic/adipogenic differentiation of BMSCs contributed to
242 GONFH.

243 BMSCs are a group of heterogeneous cells, and their majorities are derived from skeletal
244 progenitors*(Gao et al., 2021)*. It has reported that both $Col2^+$ progenitors and Osx^+ progenitors
245 provide a large proportion of BMSCs*(Ono et al., 2014)*. Adult transgenic mice with conditional
246 deletion of *β-catenin* in $Col2^+$ cells, but not Osx^+ cells, displayed a GONFH-like phenotype.
247 Extensive trabecular bone were replaced by fat droplets in the femoral head (especially in the
248 subchondral bone region) of *β-catenin*^{Col2ER} mice compared to *β-catenin*^{OsxER} mice. Cell fate
249 mapping revealed a apparent difference in the distributions of Osx^+ cells and $Col2^+$ cells in the
250 femoral head when mice induced at 2-week-old. Besides of the similar parts with Osx^+ cells
251 (osteoblasts, osteocytes and stromal cells underneath growth plate), $Col2^+$ cells also largely
252 expressed in the chondrocytes of articular cartilage, secondary ossification center and growth plate.
253 Whether these $Col2^+$ chondrocytes in secondary ossification center and growth plate caused this
254 GONFH-like phenotype, as it has been reported that the osteogenic commitment of these $Col2^+$
255 chondrocytes*(Shu et al., 2021; Li et al., 2022)*. At the age of 3 month, $Col2^+$ chondrocytes in the
256 secondary ossification center and growth plate were almost replaced by $Col2^+$ osteoblasts,
257 osteocytes and stromal cells, while GONFH-like phenotype including fat droplets accumulation
258 and sparse bone trabeculae could be still observed in 6-month-old β-catenin^{Col2ER} mice, indicating
259 that not only $Col2^+$ chondrocytes but all $Col2^+$ cells in different cellular morphology were
260 involved in this GONFH-like phenotype. Nine months of lineage trace further revealed that $Col2^+$
261 cells had self-renew ability and could continuously produced osteoblasts. The decreased ALP,
262 Runx2 and increased CEBP/α and PPAR-γ in *β-catenin*^{Col2ER} mice revealed that deletion of
263 *β-catenin* shifted the commitment of $Col2^+$ cells from osteoblasts to adipocytes, which should be
264 responsible for this GONFH-like phenotype.

265 Femoral head collapse is the key feature of late stage GONFH and is disastrous to hip
266 joint*(Wang et al., 2019b)*. Although it has been well recognized that poor mechanical supports
267 caused structural collapse of necrotic femoral head*(Fan et al., 2011)*, its detailed pathogenesis is
268 poorly understood due to lack of ideal animal models. Glucocorticoid-induced bipedal and

quadrupedal animal models only exhibit the early necrotic changes of GONFH*(Xu et al., 2018)*, without structure collapse of femoral head in MPS-induced rats. Other models using chemical or physical approaches are all failed to mimic full-range osteonecrosis of GONFH in humans*(Wang et al., 2021)*. Importantly, we found that femoral head collapse occurred spontaneously in older *β-catenin*^{Col2ER} mice. Besides the early necrotic changes including trabecular bone loss, empty lacunae and fat droplets accumulation, extensive subchondral bone destruction were identified in 6-month-old *β-catenin*^{Col2ER} mice. Previous studies have revealed that strong trabeculae and integrated subchondral bone are critical to maintain femoral head morphology*(Kawano et al., 2020; Motomura et al., 2011)*. A significant decrease of loading-bearing stiffness confirmed a poor biomechanical supports in 6-month-old *β-catenin*^{Col2ER} mice. Therefore, it could be concluded that β-catenin inhibition-induced imbalanced osteogenic/adipogenic differentiation of Col2^{+} cells caused a poor biomechanical supports (manifesting with sparse trabeculae and subchondral bone destruction), eventually leading to femoral head collapse in *β-catenin*^{Col2ER} mice.

Osteocytes are the bone cells with longest life, up to decades within their mineralized environment*(Dallas et al., 2013; Bonewald, 2011)*. However, numerous empty lacunae of osteocyte were observed in the necrotic femoral head of GONFH patients and glucocorticoid-induced rats. Glucocorticoids are known to induce cell apoptosis*(Weinstein, 2012)*, and TUNEL staining confirmed increased osteocyte apoptosis in the human and rat necrotic femoral heads, leaving behinds these empty lacunae. The importance of β-catenin in the regulation of apoptosis is well established in skeletal system*(Jähn et al., 2012; Kitase et al., 2010)*. Consistently, the expression of β-catenin was significantly decreased in the human and rat necrotic femoral heads. Moreover, we found that genetic deletion of β-catenin in Col2^{+} cells spontaneously caused osteocyte apoptosis in mice and activation of β-catenin by systematically injecting Wnt agonist 1 alleviated osteocyte apoptosis in glucocorticoid-induced rats, which indicate that β-catenin inhibition-induced osteocyte apoptosis contributed to empty lacunae of GONFH.

In summary, our studies revealed that β-catenin inhibition induces the imbalance in osteogenic/adipogenic differentiation of BMSCs and plays a crucial role in GONFH pathogenesis. We also provided a *Col2*-specific *β-catenin* knockout mouse model, for the first time, which mimics full spectrum of osteonecrosis phenotype of GONFH.

Materials and methods

299 **Human specimen collection**

300 Fifteen necrotic femoral head samples were collected from GONFH patients (ARCO grades
301 III-IV) who received arthroplasty surgery. Ten non-necrotic femoral head samples were acquired
302 from femoral neck fracture patients. All experiments with human specimens were approved by the
303 Ethics Committee of the First Affiliated Hospital of Zhejiang Chinese Medical University
304 (2018KL-005).

305 **Animals and interventions**

306 Thirty 2-month-old male Sprague-Dawley (SD) rats were purchased from the Animal
307 Laboratory Center of Zhejiang Chinese Medical University (Zhejiang, China, SCXK 2014-0004),
308 and randomly divided into the sham group, the GONFH group and the treatment group (n = 10 per
309 group). We adopted Zheng's methods to establish a glucocorticoid-induced GONFH rat
310 model*(Zheng et al., 2018)*. Firstly, rats in the GONFH group and the treatment group received
311 once injection of lipopolysaccharide (0.2 mg/kg body weight, Sigma, USA) by tail vein, followed
312 by three continuous intraperitoneal injections of 100 mg/kg body methylprednisolone (MPS,
313 Pfizer, USA). At the subsequent 6 weeks, MPS were intraperitoneally injected at the dosage of 40
314 mg/kg body weight three times every week. Rats in the treatment group were intravenously
315 injected with Wnt agonist 1 (5 mg/kg body weight, Selleck, USA) at synchronous frequency with
316 MPS.

317 *Col2-CreER*^{T2} mice, *β-catenin*$^{flox/flox}$ mice, *Osterix-CreER*^{T2} mice and *Rosa26*^{tdTomato} mice
318 were obtained from Jackson Laboratory. To map cell fate of Col2^{+} cells and Osx^{+} cells in the
319 femoral head, *Col2-CreER*^{T2}*;Rosa26*^{tdTomato} (*Tomato*^{Col2ER}) mice and
320 *Osterix-CreER*^{T2}*;Rosa26*^{tdTomato} (*Tomato*^{OsxER}) mice induced by intraperitoneally injecting with
321 tamoxifen (TM, 1 mg/10g body weight/day, diluted in corn oil) for 5 consecutive days at the age
322 of 2 or 4 weeks, and traced as long as 9-month-old. To further investigate the role of β-catenin in
323 GONFH pathogenesis, *Col2-CreER*^{T2}*;β-catenin*$^{flox/flox}$ (*β-catenin*^{Col2ER}) mice and
324 *Osterix-CreER*^{T2}*;β-catenin*$^{flox/flox}$ (*β-catenin*^{OsxER}) mice were generated and induced with 5
325 continuous injection of TM. After induction, Wnt agonist 1 (5 mg/kg body weight) was
326 intravenously injected into *β-catenin*^{Col2ER} mice three times every week until they were sacrificed
327 at the age of 3 months. All animal experiments were approved by the Animal Ethics Committee of
328 Zhejiang Chinese Medical University (No. 20190401-10).

329 **Stereomicroscopy observation and biomechanical testing**

330 Femoral head tissues harvested from human patients, glucocorticoid-induced GONFH rats,
331 *β-catenin*^{Col2ER} mice and *β-catenin*^{OsxER} mice were viewed under a stereomicroscope (Model
332 C-DSD230, Nikon, Japan) to assess their appearance characteristics. We further detected the
333 loading-bearing stiffness of femoral head samples using a biomechanical testing machine
334 (EnduraTec TestBenchTM system, Minnetonka, MN, USA) with an axial compression speed of
335 0.5 mm/min.

336 **μCT analysis**

337 Femoral head samples were scanned with a micro-computed tomography (μCT,Skyscan 1176，
338 Bruker μCT, Kontich, Belgium) at a resolution of 9 μm. Three-dimensional (3D) structure was
339 reconstructed using NRecon Software v1.6 as described previously*(Xia et al., 2019)*. The region
340 of interest was selected for morphometric analysis including bone volume fraction (BV/TV, %),
341 average trabecular thickness (Tb.Th, mm), average trabecular number (Tb.N, 1/mm), average
342 trabecular separation (Tb.Sp, mm) and subchondral bone defect area (%).

343 **Histology, immunohistochemistry and histomorphometry**

344 Femoral head tissues were processed into 3-μm-thick paraffin section or 10-μm-thick frozen
345 section as described previously*(Xia et al., 2020a)*. The paraffin sections were stained with Alcian
346 Blue Hematoxylin (ABH) / Orange G for histological analysis. The trabecular bone area (%), fat
347 droplet area (%) and empty lacuna rate (%) were measured using OsteoMetrics software (Decatur,
348 GA). The frozen sections were performed with 4',6-diamidino-2-phenylindole (DAPI) staining and
349 hematoxylin and eosin (H&E) staining for evaluating *Cre*-recombination efficiency.

350 Immunohistochemistry (IHC) assay were performed on the paraffin sections according to the
351 previously established procedures*(Xia et al., 2020b)*. Briefly, sections were immersed into 0.01 M
352 citrate buffer (Solarbio, Beijing, China) at 60℃ for 4 h to repair antigen. After washing with
353 phosphate buffer (PBS) three times, the sections were incubated with primary antibodies including
354 β-catenin (diluted 1:500, abcam, ab32572, UK), Runx2 (1:200, Abcam, ab76956, UK), alkaline
355 phosphatase (ALP, 1:200, ARIGO, ARG57422, CN), osteocalcin (OCN; diluted 1:200, Takara,
356 UK), PPAR-γ (1:300, Abcam,ab19481, UK), CEBP/α (1:400, Huabio, EM1710-20, CA) and fatty
357 acid-binding protein (FABP4, diluted 1:200, abcam, ab92501, UK) overnight at 4℃. After
358 incubation with secondary antibodies for 30 min at room temperature, tissue sections were stained

359 with diaminobenzidine (DAB) solution to detect positive staining and hematoxylin for
360 counterstaining. Mean density (IOD/Area) as the parameter of immunohistochemical quantitative
361 analysis was evaluated using Image-Pro Plus software (Media Cybernetics, Silver Spring, USA).

362 **Rat BMSCs isolation and identification**

363 BMSCs isolation were conducted as previously described*(Zhu et al., 2020)*. Briefly, bone
364 marrow cells were isolated from the proximal femur of 4-week-old SD rats. After centrifugation at
365 200g for 10 min, cells were resuspended with α-MEM (Gibco, Grand Island, NY) containing 10%
366 fetal bovine serum (FBS). By changing the medium 48 h later, no-adherent cells were removed
367 and the primary BMSCs were harvested. At 100% confluence, primary cultures were detached
368 using trypsin and subcultured at 8 x 10^3 cells/cm^2. A total of 50 μL third passage (P3) BMSCs
369 suspension (4 x 10^6/mL) were mixed with 5 μL of rat CD90-APC, rat anti-CD29-BV421, rat
370 anti-CD45-FITC or rat CD11b-PE (BD Pharmingen, Franklin Lakes, NJ, USA) in each flow
371 cytometry tube. After incubation at room temperature for 30 min followed by twice washes of a
372 standing buffer, the cells were resuspend by 500 μL staining buffer for flow cytometry analysis.

373 **Rat BMSCs intervention and staining**

374 To investigate the role of glucocorticoids on BMSCs differentiation, P3 BMSCs were
375 treated with gradient concentrations of dexamethasone (Dex, 0, 10, 10^2, 10^3, 10^4 , 10^5 nM) with or
376 without SKL2001 (a agonist of β-catenin) for 72 h. For oil-red O staining, BMSCs were treated
377 with adipogenic medium (α-MEM containing 10% FBS, 0.25 mM methylisobutylxanthine, 5
378 μg/mL insulin, and 50 μM indomethacin) for 72 h followed by 5 μg/mL insulin alone for an
379 additional 48 h. After fixed in 4% paraformaldehyde for 10 min, BMSCs were stained in 60%
380 saturated oil-red O solution for 5 min. For ALP staining, BMSCs were treated with osteogenic
381 medium (α-MEM containing 10% FBS, 50 μg/mL ascorbic acid and 5 mM β-glycerophosphate)
382 for 14 d, fixed in 4% paraformaldehyde for 10 min and stained with ALP staining kit (Thermo
383 Fisher Scientific, Rockford, IL, USA) for 15 min.

384 **Western blot analysis**

385 According to the appearance and CT images, two piece (about 2*2*2 cm^3) of necrotic tissues
386 were cut from each human necrotic femoral head, and the corresponding region from human
387 fractured femoral head. These necrotic and non-necrotic tissues were mixed and ground into
388 powder after processed by liquid nitrogen, respectively. Tissue powder and rat P3 BMSCs were

389 lysed by protein extraction reagent, and the liquid supernatant containing total protein was
390 obtained through centrifuging at 12000 g for 20 min. Then, proteins were separated by SDS-PAGE
391 and transferred onto nitrocellulose membranes. The membrane were incubated overnight with
392 primary antibodies including β-catenin, Runx2, Osterix, ALP, PPAR-γ and CEBP/α at 1:1000
393 dilution. Next, the membranes were incubated with appropriate horseradish peroxidase-conjugated
394 secondary antibodies at 37℃ for 1 h. The immune complexes were detected using a
395 chemiluminescence kit and visualized via the ChemiDoc XRS Gel documentation system (Bio-rad,
396 CA). The gray intensity was measured by the software of Quantity One (Bio-Rad, CA).

397 **Statistical analysis**

398 All data were presented as mean ± standard deviation (SD). Statistical analyses including
399 unpaired Student's *t*-test (two groups) and one-way ANOVA followed by Tukey's test (multiple
400 groups) were performed with the software of SPSS 22.0 software. *P<0.05, **P<0.01 was
401 considered statistically significant.

Data Availability Statement

Raw data are mainly attached in the current study. Any other data involving this study are available from the corresponding author upon request.

Acknowledgements

This work has been supported by Chinese National Natural Science Foundation (grants nos. 81873325, 82074469, 82104885), Natural Science Foundation of Zhejiang Province (grant no. Q22H271191), Ningbo medical key discipline (No. 2022-B01).

Author Contributions

Di Chen, Chenjie Xia and Hongting Jin conceived this study. Chenjie Xia wrote the paper. Di Chen and Hongting Jin revised the paper. Chenjie Xia, Huihui Xu, Ping-er Wang, Liang Fang, Jiali Chen, Wenhua Yuan, Danqing Fu, Xucheng Wang performed the experiments and analyzed the data. Bangjian He, Luwei Xiao, Peijian Tong and Chengliang Wu collected the human samples.

Declaration of Interests

Competing interests: The authors declare no competing interests.

402

References

Bonewald LF. 2011. The amazing osteocyte. *Journal of bone and mineral research : the official journal of the American Society for Bone and Mineral Research* **26**:229-238. doi: 10.1002/jbmr.320, PMID: 21254230

Cao Y, Jiang C, Wang X, Wang H, Yan Z, Yuan H. 2021. Reciprocal effect of microRNA-224 on osteogenesis and

adipogenesis in steroid-induced osteonecrosis of the femoral head. *Bone* **145**:115844. doi: 10.1016/j.bone.2021.115844, PMID: 33453444

Chang CC, Greenspan A, Gershwin ME. 1993. Osteonecrosis: current perspectives on pathogenesis and treatment. *Seminars in arthritis and rheumatism* **23**:47-69. doi: 10.1016/s0049-0172(05)80026-5, PMID: 8235665

Chen CY, Rao SS, Yue T, Tan YJ, Yin H, Chen LJ, Luo MJ, Wang Z, Wang YY, Hong CG, Qian YX, He ZH, Liu JH, Yang F, Huang FY, Tang SY, Xie H. 2022. Glucocorticoid-induced loss of beneficial gut bacterial extracellular vesicles is associated with the pathogenesis of osteonecrosis. *Science advances* **8**:eabg8335. doi: 10.1126/sciadv.abg8335, PMID: 35417243

Chen G, Wang Q, Li Z, Yang Q, Liu Y, Du Z, Zhang G, Song Y. 2020. Circular RNA CDR1as promotes adipogenic and suppresses osteogenic differentiation of BMSCs in steroid-induced osteonecrosis of the femoral head. *Bone* **133**:115258. doi: 10.1016/j.bone.2020.115258, PMID: 32018039

Chen XJ, Shen YS, He MC, Yang F, Yang P, Pang FX, He W, Cao YM, Wei QS. 2019. Polydatin promotes the osteogenic differentiation of human bone mesenchymal stem cells by activating the BMP2-Wnt/β-catenin signaling pathway. *Biomedicine & pharmacotherapy = Biomedecine & pharmacotherapie* **112**:108746. doi: 10.1016/j.biopha.2019.108746, PMID: 30970530

Dallas SL, Prideaux M, Bonewald LF. 2013. The osteocyte: an endocrine cell ... and more. *Endocrine reviews* **34**:658-690. doi: 10.1210/er.2012-1026, PMID: 23612223

Fan M, Peng J, Qin L, Lu S. 2011. Experimental animal models of osteonecrosis. *Rheumatology international* **31**:983-994. doi: 10.1007/s00296-011-1819-9, PMID: 21340568

Fang S, Li Y, Chen P. 2019. Osteogenic effect of bone marrow mesenchymal stem cell-derived exosomes on steroid-induced osteonecrosis of the femoral head. *Drug design, development and therapy* **13**:45-55. doi: 10.2147/DDDT.S178698, PMID: 30587927

Feng X, Xiang Q, Jia J, Guo T, Liao Z, Yang S, Cai X, Liu X. 2022. CircHGF suppressed cell proliferation and osteogenic differentiation of BMSCs in ONFH via inhibiting miR-25-3p binding to SMAD7. *Molecular therapy. Nucleic acids* **28**:99-113. doi: 10.1016/j.omtn.2022.02.017, PMID: 35402073

Gangji V, Hauzeur JP. 2005. Treatment of osteonecrosis of the femoral head with implantation of autologous bone-marrow cells. Surgical technique. *The Journal of bone and joint surgery. American volume* **87 Suppl 1**:106-112. doi: 10.2106/JBJS.D.02662, PMID: 15743852

Gao Q, Wang L, Wang S, Huang B, Jing Y, Su J. 2021. Bone Marrow Mesenchymal Stromal Cells: Identification, Classification, and Differentiation. *Frontiers in cell and developmental biology* **9**:787118. doi: 10.3389/fcell.2021.787118, PMID: 35047499

Gu C, Xu Y, Zhang S, Guan H, Song S, Wang X, Wang Y, Li Y, Zhao G. 2016. miR-27a attenuates adipogenesis and promotes osteogenesis in steroid-induced rat BMSCs by targeting PPARγ and GREM1. *Scientific reports* **6**:38491. doi: 10.1038/srep38491, PMID: 27910957

Guzman RA, Maruyama M, Moeinzadeh S, Lui E, Zhang N, Storaci HW, Tam K, Huang EE, Utsunomiya T, Rhee C, Gao Q, Yao Z, Yang YP, Goodman SB. 2021. The effect of genetically modified platelet-derived growth factor-BB over-expressing mesenchymal stromal cells during core decompression for steroid-associated osteonecrosis of the femoral head in rabbits. *Stem cell research & therapy* **12**:503. doi: 10.1186/s13287-021-02572-7, PMID: 34526115

Han L, Wang B, Wang R, Gong S, Chen G, Xu W. 2019. The shift in the balance between osteoblastogenesis and adipogenesis of mesenchymal stem cells mediated by glucocorticoid receptor. *Stem cell research & therapy* **10**:377. doi: 10.1186/s13287-019-1498-0, PMID: 31805987

Hines JT, Jo WL, Cui Q, Mont MA, Koo KH, Cheng EY, Goodman SB, Ha YC, Hernigou P, Jones LC, Kim SY, Sakai T, Sugano N, Yamamoto T, Lee MS, Zhao D, Drescher W, Kim TY, Lee YK, Yoon BH, Baek SH,

Ando W, Kim HS, Park JW. 2021. Osteonecrosis of the Femoral Head: an Updated Review of ARCO on Pathogenesis, Staging and Treatment. *Journal of Korean medical science* **36**:e177. doi: 10.3346/jkms.2021.36.e177, PMID: 34155839

Houdek MT, Wyles CC, Packard BD, Terzic A, Behfar A, Sierra RJ. 2016. Decreased Osteogenic Activity of Mesenchymal Stem Cells in Patients With Corticosteroid-Induced Osteonecrosis of the Femoral Head. *The Journal of arthroplasty* **31**:893-898. doi: 10.1016/j.arth.2015.08.017, PMID: 26404846

Jähn K, Lara-Castillo N, Brotto L, Mo CL, Johnson ML, Brotto M, Bonewald LF. 2012. Skeletal muscle secreted factors prevent glucocorticoid-induced osteocyte apoptosis through activation of β-catenin. *European cells & materials* **24**:197-209; discussion 209-210. doi: 10.22203/ecm.v024a14, PMID: 22972510

Kawano K, Motomura G, Ikemura S, Yamaguchi R, Baba S, Xu M, Nakashima Y. 2020. Differences in the microarchitectural features of the lateral collapsed lesion between osteonecrosis and subchondral insufficiency fracture of the femoral head. *Bone* **141**:115585. doi: 10.1016/j.bone.2020.115585, PMID: 32795680

Kitase Y, Barragan L, Qing H, Kondoh S, Jiang JX, Johnson ML, Bonewald LF. 2010. Mechanical induction of PGE2 in osteocytes blocks glucocorticoid-induced apoptosis through both the β-catenin and PKA pathways. *Journal of bone and mineral research : the official journal of the American Society for Bone and Mineral Research* **25**:2657-2668. doi: 10.1002/jbmr.168, PMID: 20578217

Lavernia CJ, Sierra RJ, Grieco FR. 1999. Osteonecrosis of the femoral head. *The Journal of the American Academy of Orthopaedic Surgeons* **7**:250-261. doi: 10.5435/00124635-199907000-00005, PMID: 10434079

Lee JS, Lee JS, Roh HL, Kim CH, Jung JS, Suh KT. 2006. Alterations in the differentiation ability of mesenchymal stem cells in patients with nontraumatic osteonecrosis of the femoral head: comparative analysis according to the risk factor. *Journal of orthopaedic research : official publication of the Orthopaedic Research Society* **24**:604-609. doi: 10.1002/jor.20078, PMID: 16514658

Li L, Wang Y, Yu X, Bao Y, An L, Wei X, Yu W, Liu B, Li J, Yang J, Xia Y, Liu G, Cao F, Zhang X, Zhao D. 2020. Bone marrow mesenchymal stem cell-derived exosomes promote plasminogen activator inhibitor 1 expression in vascular cells in the local microenvironment during rabbit osteonecrosis of the femoral head. *Stem cell research & therapy* **11**:480. doi: 10.1186/s13287-020-01991-2, PMID: 33176873

Li X, Yang S, Yuan G, Jing D, Qin L, Zhao H, Yang S. 2022. Type II collagen-positive progenitors are important stem cells in controlling skeletal development and vascular formation. *Bone research* **10**:46. doi: 10.1038/s41413-022-00214-z, PMID: 35739091

Liu Y, Strecker S, Wang L, Kronenberg MS, Wang W, Rowe DW, Maye P. 2013. Osterix-cre labeled progenitor cells contribute to the formation and maintenance of the bone marrow stroma. *PloS one* **8**:e71318. doi: 10.1371/journal.pone.0071318, PMID: 23951132

Motomura G, Yamamoto T, Yamaguchi R, Ikemura S, Nakashima Y, Mawatari T, Iwamoto Y. 2011. Morphological analysis of collapsed regions in osteonecrosis of the femoral head. *The Journal of bone and joint surgery. British volume* **93**:184-187. doi: 10.1302/0301-620X.93B225476, PMID: 21282756

Ono N, Ono W, Nagasawa T, Kronenberg HM. 2014. A subset of chondrogenic cells provides early mesenchymal progenitors in growing bones. *Nature cell biology* **16**:1157-1167. doi: 10.1038/ncb3067, PMID: 25419849

Petek D, Hannouche D, Suva D. 2019. Osteonecrosis of the femoral head: pathophysiology and current concepts of treatment. *EFORT open reviews* **4**:85-97. doi: 10.1302/2058-5241.4.180036, PMID: 30993010

Qin L, Yao D, Zheng L, Liu WC, Liu Z, Lei M, Huang L, Xie X, Wang X, Chen Y, Yao X, Peng J, Gong H, Griffith JF, Huang Y, Zheng Y, Feng JQ, Liu Y, Chen S, Xiao D, Wang D, Xiong J, Pei D, Zhang P, Pan X, Wang X, Lee KM, Cheng CY. 2015. Phytomolecule icaritin incorporated PLGA/TCP scaffold for

steroid-associated osteonecrosis: Proof-of-concept for prevention of hip joint collapse in bipedal emus and mechanistic study in quadrupedal rabbits. *Biomaterials* **59**:125-143. doi: 10.1016/j.biomaterials.2015.04.038, PMID: 25968462

Rackwitz L, Eden L, Reppenhagen S, Reichert JC, Jakob F, Walles H, Pullig O, Tuan RS, Rudert M, Nöth U. 2012. Stem cell- and growth factor-based regenerative therapies for avascular necrosis of the femoral head. *Stem cell research & therapy* **3**:7. doi: 10.1186/scrt98, PMID: 22356811

Scaglione M, Fabbri L, Celli F, Casella F, Guido G. 2015. Hip replacement in femoral head osteonecrosis: current concepts. *Clinical cases in mineral and bone metabolism : the official journal of the Italian Society of Osteoporosis, Mineral Metabolism, and Skeletal Diseases* **12**:51-54. doi: 10.11138/ccmbm/2015.12.3s.051, PMID: 27134633

Shu HS, Liu YL, Tang XT, Zhang XS, Zhou B, Zou W, Zhou BO. 2021. Tracing the skeletal progenitor transition during postnatal bone formation. *Cell stem cell* **28**:2122-2136.e3. doi: 10.1016/j.stem.2021.08.010, PMID: 34499868

Song L, Liu M, Ono N, Bringhurst FR, Kronenberg HM, Guo J. 2012. Loss of wnt/ β -catenin signaling causes cell fate shift of preosteoblasts from osteoblasts to adipocytes. *Journal of bone and mineral research : the official journal of the American Society for Bone and Mineral Research* **27**:2344-2358. doi: 10.1002/jbmr.1694, PMID: 22729939

Sun H, Zhang W, Yang N, Xue Y, Wang T, Wang H, Zheng K, Wang Y, Zhu F, Yang H, Xu W, Xu Y, Geng D. 2021. Activation of cannabinoid receptor 2 alleviates glucocorticoid-induced osteonecrosis of femoral head with osteogenesis and maintenance of blood supply. *Cell death & disease* **12**:1035. doi: 10.1038/s41419-021-04313-3, PMID: 34718335

Tabatabaee RM, Saberi S, Parvizi J, Mortazavi SM, Farzan M. 2015. Combining Concentrated Autologous Bone Marrow Stem Cells Injection With Core Decompression Improves Outcome for Patients with Early-Stage Osteonecrosis of the Femoral Head: A Comparative Study. *The Journal of arthroplasty* **30**:11-15. doi: 10.1016/j.arth.2015.06.022, PMID: 26143238

Takada I, Kouzmenko AP, Kato S. 2009. Wnt and PPARgamma signaling in osteoblastogenesis and adipogenesis. *Nature reviews. Rheumatology* **5**:442-447. doi: 10.1038/nrrheum.2009.137, PMID: 19581903

Tao SC, Yuan T, Rui BY, Zhu ZZ, Guo SC, Zhang CQ. 2017. Exosomes derived from human platelet-rich plasma prevent apoptosis induced by glucocorticoid-associated endoplasmic reticulum stress in rat osteonecrosis of the femoral head via the Akt/Bad/Bcl-2 signal pathway. *Theranostics* **7**:733-750. doi: 10.7150/thno.17450, PMID: 28255363

Tencerova M, Kassem M. 2016. The Bone Marrow-Derived Stromal Cells: Commitment and Regulation of Adipogenesis. *Frontiers in endocrinology* **7**:127. doi: 10.3389/fendo.2016.00127, PMID: 27708616

Wang A, Ren M, Wang J. 2018b. The pathogenesis of steroid-induced osteonecrosis of the femoral head: A systematic review of the literature. *Gene* **671**:103-109. doi: 10.1016/j.gene.2018.05.091, PMID: 29859289

Wang BL, Sun W, Shi ZC, Lou JN, Zhang NF, Shi SH, Guo WS, Cheng LM, Ye LY, Zhang WJ, Li ZR. 2008. Decreased proliferation of mesenchymal stem cells in corticosteroid-induced osteonecrosis of femoral head. *Orthopedics* **31**:444. doi: 10.3928/01477447-20080501-33, PMID: 19292322

Wang C, Meng H, Wang Y, Zhao B, Zhao C, Sun W, Zhu Y, Han B, Yuan X, Liu R, Wang X, Wang A, Guo Q, Peng J, Lu S. 2018a. Analysis of early stage osteonecrosis of the human femoral head and the mechanism of femoral head collapse. *International journal of biological sciences* **14**:156-164. doi: 10.7150/ijbs.18334, PMID: 29483834

Wang C, Sun W, Ling S, Wang Y, Wang X, Meng H, Li Y, Yuan X, Li J, Liu R, Zhao D, Lu Q, Wang A, Guo Q, Lu S, Tian H, Li Y, Peng J. 2019b. AAV-Anti-miR-214 Prevents Collapse of the Femoral Head in

Osteonecrosis by Regulating Osteoblast and Osteoclast Activities. *Molecular therapy. Nucleic acids* **18**:841-850. doi: 10.1016/j.omtn.2019.09.030, PMID: 31739209

Wang C, Wu Z, Li X, Shi L, Xie Q, Liu D, Guo Z, Zheng W. 2021. An animal model of early-stage femoral head osteonecrosis induced by cryo-insult in small tailed Han sheep. *Journal of orthopaedic translation* **26**:84-91. doi: 10.1016/j.jot.2020.06.004, PMID: 33437627

Wang Q, Yang Q, Chen G, Du Z, Ren M, Wang A, Zhao H, Li Z, Zhang G, Song Y. 2018c. LncRNA expression profiling of BMSCs in osteonecrosis of the femoral head associated with increased adipogenic and decreased osteogenic differentiation. *Scientific reports* **8**:9127. doi: 10.1038/s41598-018-27501-2, PMID: 29904151

Wang Y, Luan S, Yuan Z, Lin C, Fan S, Wang S, Ma C, Wu S. 2022. Therapeutic effect of platelet-rich plasma on glucocorticoid-induced rat bone marrow mesenchymal stem cells in vitro. *BMC musculoskeletal disorders* **23**:151. doi: 10.1186/s12891-022-05094-2, PMID: 35168574

Wang Z, Sun QM, Zhang FQ, Zhang QL, Wang LG, Wang WJ. 2019a. Core decompression combined with autologous bone marrow stem cells versus core decompression alone for patients with osteonecrosis of the femoral head: A meta-analysis. *International journal of surgery (London, England)* **69**:23-31. doi: 10.1016/j.ijsu.2019.06.016, PMID: 31301432

Weinstein RS. 2012. Glucocorticoid-induced osteonecrosis. *Endocrine* **41**:183-190. doi: 10.1007/s12020-011-9580-0, PMID: 22169965

Xia C, Ge Q, Fang L, Yu H, Zou Z, Zhang P, Lv S, Tong P, Xiao L, Chen D, Wang PE, Jin H. 2020a. TGF-β/Smad2 signalling regulates enchondral bone formation of Gli1+ periosteal cells during fracture healing. *Cell proliferation* **53**:e12904. doi: 10.1111/cpr.12904, PMID: 32997394

Xia C, Wang P, Fang L, Ge Q, Zou Z, Dong R, Zhang P, Shi Z, Xu R, Zhang L, Luo C, Ying J, Xiao L, Shen J, Chen D, Tong P, Jin H. 2019. Activation of β-catenin in Col2-expressing chondrocytes leads to osteoarthritis-like defects in hip joint. *Journal of cellular physiology* **234**:18535-18543. doi: 10.1002/jcp.28491, PMID: 30912140

Xia C, Zou Z, Fang L, Ge Q, Zhang P, Xu H, Xu R, Shi Z, Lin H, Ding X, Xiao L, Tong P, Wang PE, Jin H. 2020b. Bushenhuoxue formula promotes osteogenic differentiation of growth plate chondrocytes through β-catenin-dependent manner during osteoporosis. *Biomedicine & pharmacotherapy = Biomedecine & pharmacotherapie* **127**:110170. doi: 10.1016/j.biopha.2020.110170, PMID: 32334373

Xiang S, Li Z, Weng X. 2020. Changed cellular functions and aberrantly expressed miRNAs and circRNAs in bone marrow stem cells in osteonecrosis of the femoral head. *International journal of molecular medicine* **45**:805-815. doi: 10.3892/ijmm.2020.4455, PMID: 31922208

Xu C, Wang J, Zhu T, Shen Y, Tang X, Fang L, Xu Y. 2016. Cross-Talking Between PPAR and WNT Signaling and its Regulation in Mesenchymal Stem Cell Differentiation. *Current stem cell research & therapy* **11**:247-254. doi: 10.2174/1574888x10666150723145707, PMID: 26201865

Xu HH, Li SM, Fang L, Xia CJ, Zhang P, Xu R, Shi ZY, Zou Z, Ge QW, Wang P, Tong PJ, Jin HT. 2021. Platelet-rich plasma promotes bone formation, restrains adipogenesis and accelerates vascularization to relieve steroids-induced osteonecrosis of the femoral head. *Platelets* **32**:950-959. doi: 10.1080/09537104.2020.1810221, PMID: 32835568

Xu J, Gong H, Lu S, Deasey MJ, Cui Q. 2018. Animal models of steroid-induced osteonecrosis of the femoral head-a comprehensive research review up to 2018. *International orthopaedics* **42**:1729-1737. doi: 10.1007/s00264-018-3956-1, PMID: 29705870

Xu Y, Jiang Y, Wang Y, Jia B, Gao S, Yu H, Zhang H, Lv C, Li H, Li T. 2022. LINC00473-modified bone marrow mesenchymal stem cells incorporated thermosensitive PLGA hydrogel transplantation for steroid-induced

osteonecrosis of femoral head: A detailed mechanistic study and validity evaluation. *Bioengineering & translational medicine* **7**:e10275. doi: 10.1002/btm2.10275, PMID: 35600648

Yang N, Sun H, Xue Y, Zhang W, Wang H, Tao H, Liang X, Li M, Xu Y, Chen L, Zhang L, Huang L, Geng D. 2021. Inhibition of MAGL activates the Keap1/Nrf2 pathway to attenuate glucocorticoid-induced osteonecrosis of the femoral head. *Clinical and translational medicine* **11**:e447. doi: 10.1002/ctm2.447, PMID: 34185425

Yin L, Li YB, Wang YS. 2006. Dexamethasone-induced adipogenesis in primary marrow stromal cell cultures: mechanism of steroid-induced osteonecrosis. *Chinese medical journal* **119**:581-588. PMID: 16620700

Yu Z, Fan L, Li J, Ge Z, Dang X, Wang K. 2016. Lithium prevents rat steroid-related osteonecrosis of the femoral head by β-catenin activation. *Endocrine* **52**:380-390. doi: 10.1007/s12020-015-0747-y, PMID: 26458922

Yuan Z, Li Q, Luo S, Liu Z, Luo D, Zhang B, Zhang D, Rao P, Xiao J. 2016. PPARγ and Wnt Signaling in Adipogenic and Osteogenic Differentiation of Mesenchymal Stem Cells. *Current stem cell research & therapy* **11**:216-225. doi: 10.2174/1574888x10666150519093429, PMID: 25986621

Zaidi M, Sun L, Robinson LJ, Tourkova IL, Liu L, Wang Y, Zhu LL, Liu X, Li J, Peng Y, Yang G, Shi X, Levine A, Iqbal J, Yaroslavskiy BB, Isales C, Blair HC. 2010. ACTH protects against glucocorticoid-induced osteonecrosis of bone. *Proceedings of the National Academy of Sciences of the United States of America* **107**:8782-8787. doi: 10.1073/pnas.0912176107, PMID: 20421485

Zalavras C, Shah S, Birnbaum MJ, Frenkel B. 2003. Role of apoptosis in glucocorticoid-induced osteoporosis and osteonecrosis. *Critical reviews in eukaryotic gene expression* **13**:221-235. PMID: 14696969

Zhang C, Zou YL, Ma J, Dang XQ, Wang KZ. 2015. Apoptosis associated with Wnt/β-catenin pathway leads to steroid-induced avascular necrosis of femoral head. *BMC musculoskeletal disorders* **16**:132. doi: 10.1186/s12891-015-0606-2, PMID: 26037065

Zhang P, Xu H, Wang P, Dong R, Xia C, Shi Z, Xu R, Fang L, Zou Z, Ge Q, Tong P, Jin H. 2019. Yougui pills exert osteoprotective effects on rabbit steroid-related osteonecrosis of the femoral head by activating β-catenin. *Biomedicine & pharmacotherapy = Biomedecine & pharmacotherapie* **120**:109520. doi: 10.1016/j.biopha.2019.109520, PMID: 31629251

Zhang XY, Li HN, Chen F, Chen YP, Chai Y, Liao JZ, Gan B, Chen DP, Li S, Liu YQ. 2021. Icariin regulates miR-23a-3p-mediated osteogenic differentiation of BMSCs via BMP-2/Smad5/Runx2 and WNT/β-catenin pathways in osteonecrosis of the femoral head. *Saudi pharmaceutical journal : SPJ : the official publication of the Saudi Pharmaceutical Society* **29**:1405-1415. doi: 10.1016/j.jsps.2021.10.009, PMID: 35002378

Zhao D, Zhang F, Wang B, Liu B, Li L, Kim SY, Goodman SB, Hernigou P, Cui Q, Lineaweaver WC, Xu J, Drescher WR, Qin L. 2020. Guidelines for clinical diagnosis and treatment of osteonecrosis of the femoral head in adults (2019 version). *Journal of orthopaedic translation* **21**:100-110. doi: 10.1016/j.jot.2019.12.004, PMID: 32309135

Zhao H, Yeersheng R, Xia Y, Kang P, Wang W. 2021. Hypoxia Enhanced Bone Regeneration Through the HIF-1α/β-Catenin Pathway in Femoral Head Osteonecrosis. *The American journal of the medical sciences* **362**:78-91. doi: 10.1016/j.amjms.2021.03.005, PMID: 33727018

Zheng LZ, Wang JL, Kong L, Huang L, Tian L, Pang QQ, Wang XL, Qin L. 2018. Steroid-associated osteonecrosis animal model in rats. *Journal of orthopaedic translation* **13**:13-24. doi: 10.1016/j.jot.2018.01.003, PMID: 29662787

Zhu W, Guo M, Yang W, Tang M, Chen T, Gan D, Zhang D, Ding X, Zhao A, Zhao P, Yan W, Zhang J. 2020. CD41-deficient exosomes from non-traumatic femoral head necrosis tissues impair osteogenic differentiation and migration of mesenchymal stem cells. *Cell death & disease* **11**:293. doi:

10.1038/s41419-020-2496-y, PMID: 32341357

List of Figure Captions

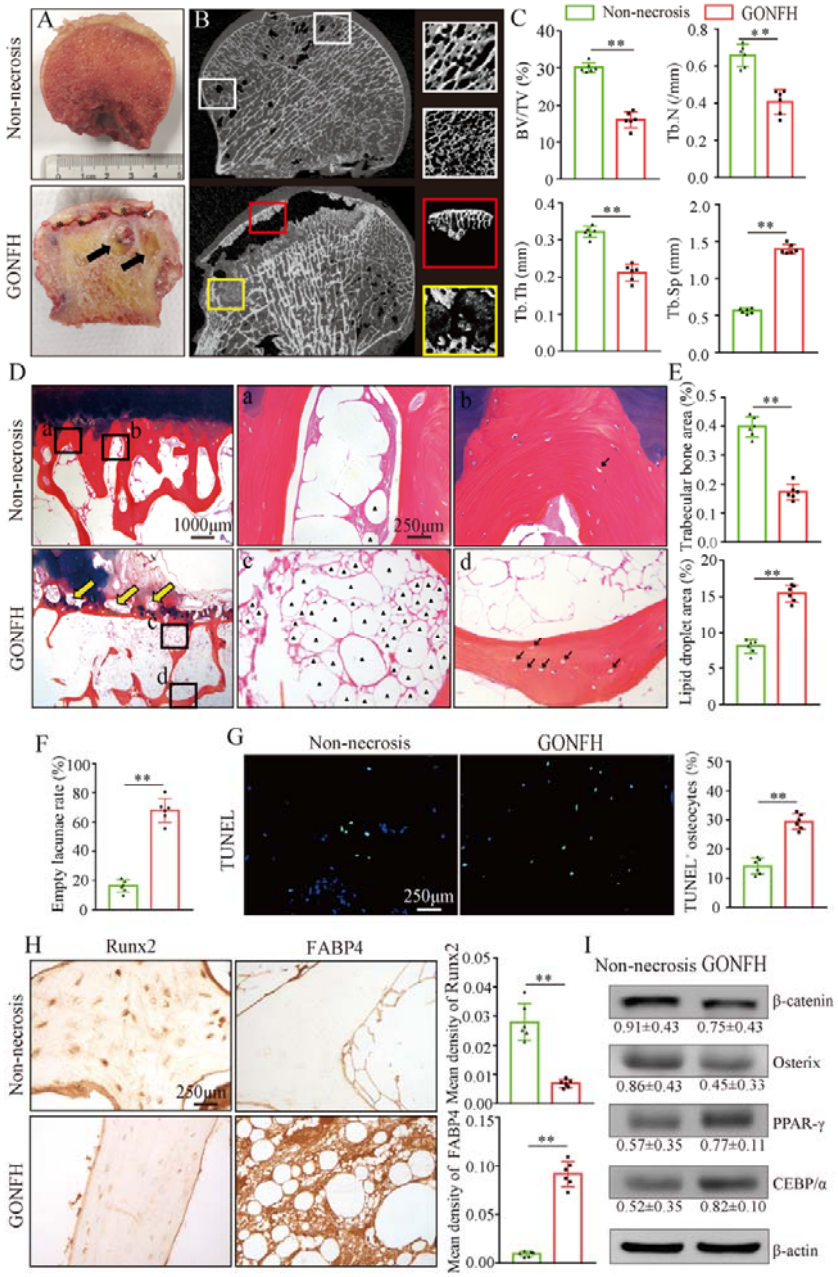

Figure 1. Abnormal osteogenesis and adipogenesis with decreased β-catenin signaling in the necrotic femoral heads of GONFH patients. Necrotic (n=15) and Non-necrotic (n=10) femoral head samples were obtained from the patients with GONFH or femoral neck fracture, respectively. (A) Gross anatomy analysis of human necrotic and non-necrotic femoral head samples. Black asterisks: subchondral collapsed region. Black arrows: liquefied necrotic region. (B) μCT images of human necrotic and non-necrotic femoral heads. Red and Yellow boxed area: 3D images of subchondral collapsed region and liquefied necrotic region, respectively. White boxed areas: 3D images of corresponding regions in the non-necrotic femoral heads. (C) Quantitative analysis of

BV/TV, Tb.N, Tb.Th and Tb.Sp on the necrotic regions. (D) ABH staining of human necrotic and non-necrotic femoral heads. a,c: high magnification images of bone marrow; b,d: high magnification images of bone trabeculae; Yellow arrows: subchondral bone destruction; black arrows: empty lacunae of osteocyte; black triangles: fat droplet. (E) Histomorphological quantitative analysis of trabecular bone area and fat droplet area. (F) Histomorphological quantitative analysis of empty lacunae rate. (G) TUNEL staining of osteocytes in human necrotic and non-necrotic femoral heads. (H) IHC staining of Runx2 and FABP4 expressions in human necrotic and non-necrotic femoral heads. (I) Western blot of β-catenin, Osterix, PPAR-γ and CEBP/α in human necrotic and non-necrotic femoral heads.

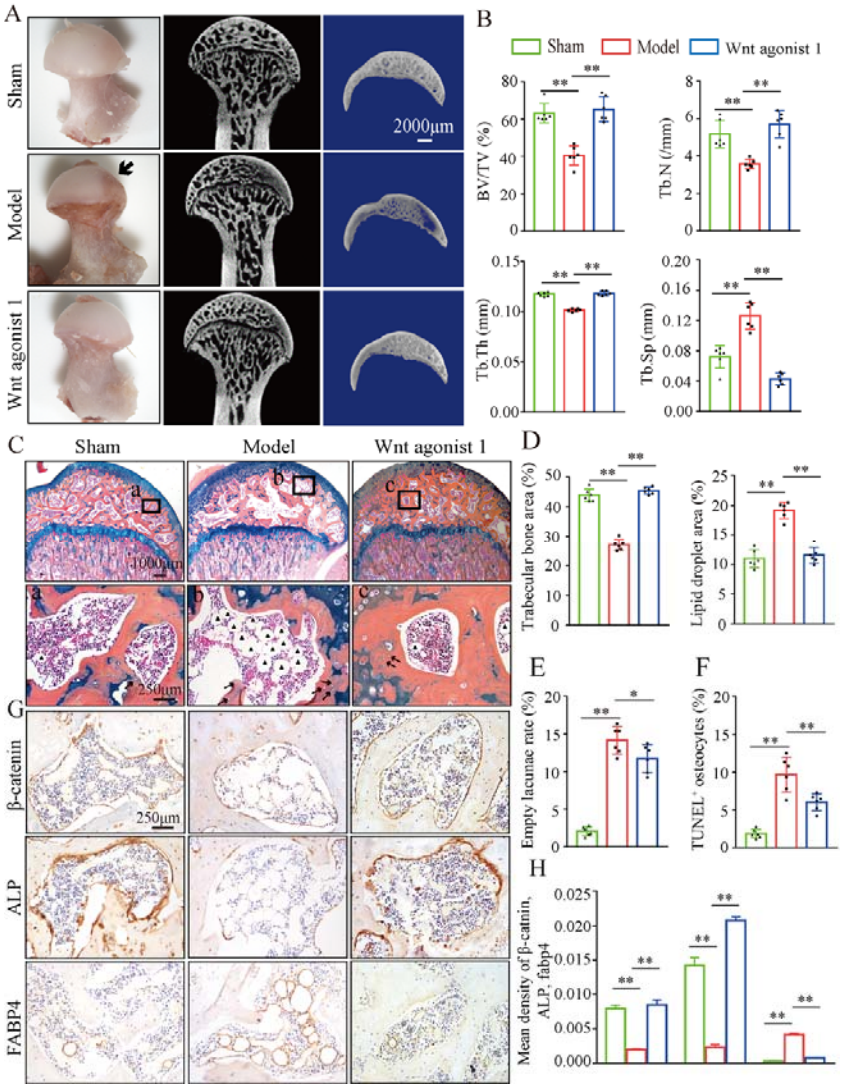

Figure 2. Systemic injection of Wnt agonist 1 alleviates abnormal osteogenesis and adipogenesis in rat GONFH femoral heads. The rat model of GONFH was established by a co-induction of lipopolysaccharide and methylprednisolone (MPS). The femoral head samples were harvested after GONFH rats were intravenously injected with Wnt agonist 1 for 6 weeks. (A) Gross anatomy analysis and μCT images of femoral heads in sham, model and Wnt agonist 1 treated groups. (B) μCT quantitative analysis of BV/TV, Tb.N, Tb.Th and Tb.Sp in each group. (C) ABH staining of

femoral heads in each group. a-c, high magnification images of the representative region; black arrows: empty lacunae of osteocyte; black triangles: fat droplet. (D) Histomorphological quantitative analysis of trabecular bone area and fat droplet area in each group. (E) Histomorphological quantitative analysis of empty lacunae rate in each group. (F) TUNEL staining of osteocytes in the femoral heads of GONFH rats. (G, H) IHC staining and quantitative analysis of β-catenin, ALP and FABP4 in rat femoral heads of each group.

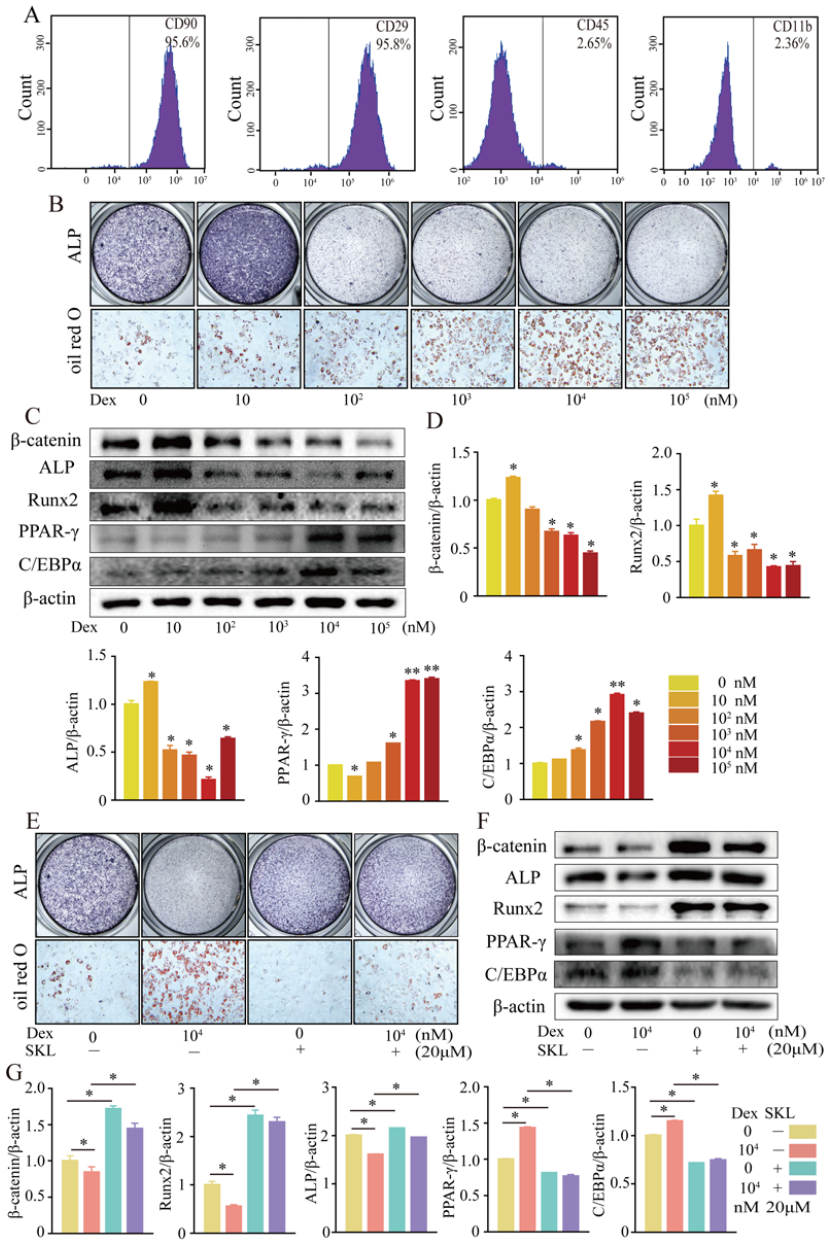

Figure 3. Activation of β-catenin redirected Dex-induced imbalanced osteogenic/adipogenic differentiation of BMSCs. Primary BMSCs were extracted from the proximal femur of 4-week-old SD rats and cultivated to passage 3 for subsequent experiments. (A) Flow cytometry analyzing the

surface markers of rat BMSCs. (B) ALP staining and oil red O staining of BMSCs at the increasing concentrations of dexamethasone (Dex). (C, D) Western blot and quantitative analysis of β-catenin, Runx2, ALP, PPAR-γ and CEBP/α in BMSCs at the increasing concentrations of Dex. (E) ALP staining and oil red O staining of rat BMSCs at the condition with or without 10^4 nM Dex and 20 μM SKL2001 (an agonist of β-catenin). (F, G) Western blot and quantitative analysis of β-catenin, Runx2, ALP, PPAR-γ and CEBP/α in rat BMSCs at the condition with or without 10^4 nM Dex and 20 μM SKL2001.

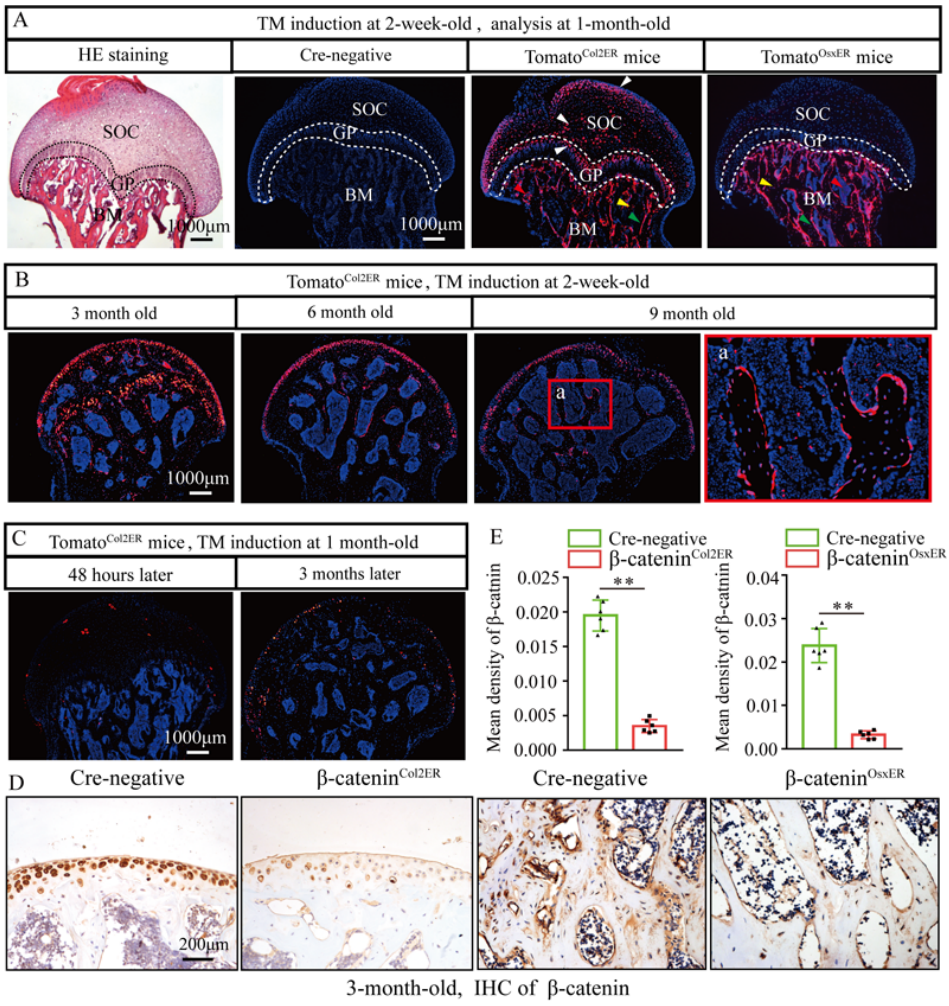

Figure 4. Fate mapping of Col2$^+$ cells and Osx$^+$ cells in the femoral head. *Tomato^{Col2ER}* mice and *Tomato^{OsxER}* mice were continuously received 5 dose of TM injections (1 mg/10 g body weight) at the age of 2 weeks for fate mapping analysis. (A) Distributions of Col2$^+$ and Osx$^+$ cells in the femoral head of 1-month-old *Tomato^{Col2ER}* mice and *Tomato^{OsxER}* mice. White arrowheads: chondrocyte; Green arrowheads: osteoblast; Yellow arrowheads: osteocyte; Red arrowheads: bone marrow stromal cell; GP: growth plate; SOC: second ossification center; BM: bone marrow. (B) Lineage trace of Col2$^+$ cells in the femoral head for 9 months. a: high magnification image of bone marrow region. (C) Poor *Cre*-recombinase efficiency in the femoral head of *Tomato^{Col2ER}* mice with TM induction at the age of 1 month. (D, E) Femoral heads were harvested from 3-month-old

β-catenin^{Col2ER} mice and *β-catenin*^{OsxER} mice to detect expression of β-catenin. IHC staining and quantitative analysis of β-catenin in the femoral heads of 3-month-old *β-catenin*^{Col2ER} mice and *β-catenin*^{OsxER} mice.

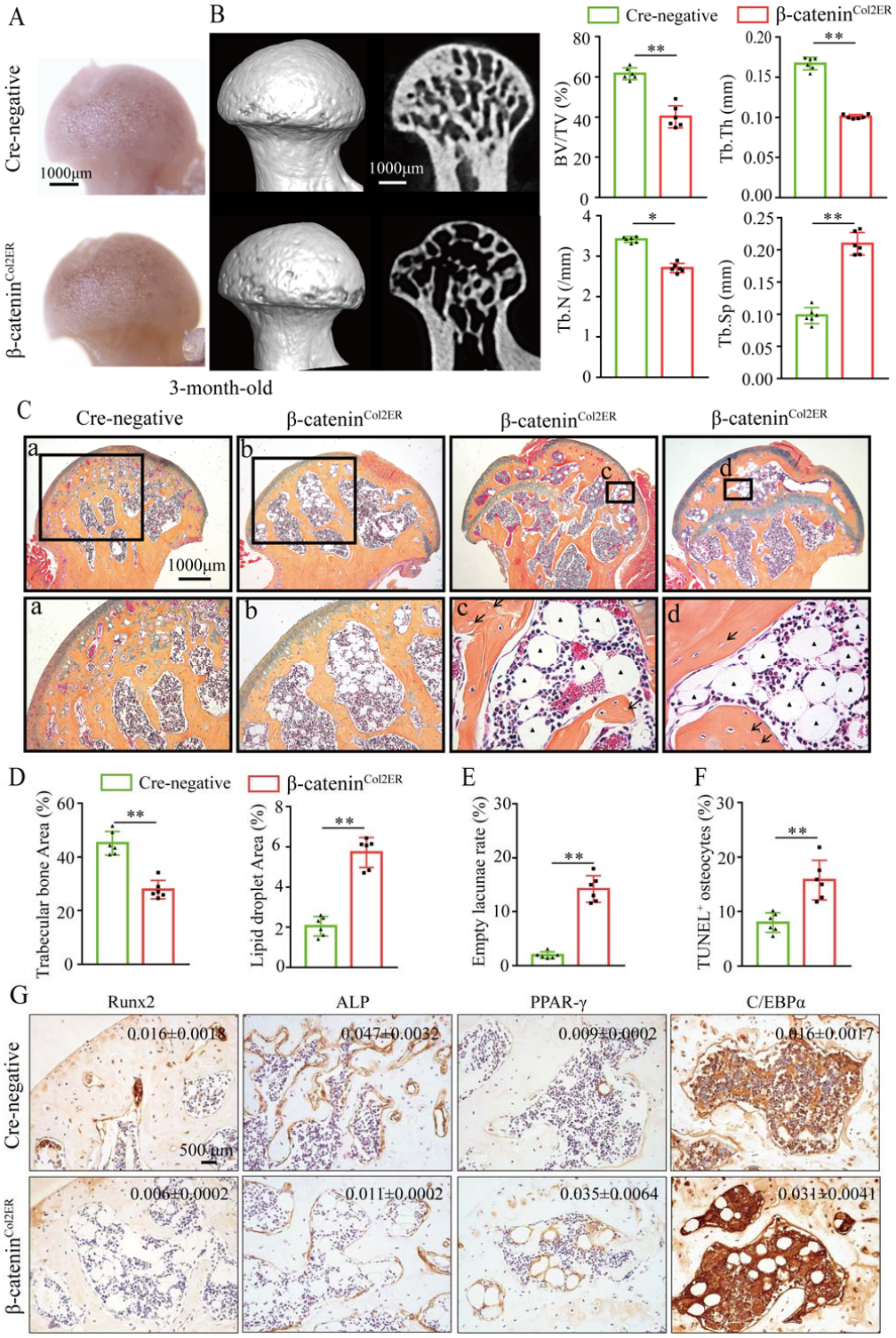

Figure 5. Deletion of *β-catenin* in Col2^{+} cells leads to a GNOFH-like phenotype. Femoral heads were harvested from 3-month-old *β-catenin*^{Col2ER} mice and *Cre*-negative littermates with 5 continuous dosage of TM injections (1 mg/10 g body weight) at the age of 2 weeks. (A) Gross anatomy analysis of femoral heads in *β-catenin*^{Col2ER} mice and *Cre*-negative littermates. (B) Representative μCT images and quantitative analysis of BV/TV, Tb. N, Tb. Th and Tb. Sp in the femoral heads of *β-catenin*^{Col2ER} mice. (C) ABH staining of femoral heads in *β-catenin*^{Col2ER} mice. a-d: high magnification images of representative subchondral bone region; Black triangle arrowheads: fat droplet; Black arrows: empty lacunae of osteocyte. (D) Histomorphological quantitative analysis of trabecular bone area and fat droplet area in the femoral heads of *β-catenin*^{Col2ER} mice. (E) Histomorphological quantitative analysis of empty lacunae rate in the femoral heads of *β-catenin*^{Col2ER} mice. (F) TUNEL staining of osteocytes in the femoral heads of *β-catenin*^{Col2ER} mice. (G) IHC staining and quantitative analysis of Runx2, ALP, PPAR-γ and CEBP/α in the femoral heads of *β-catenin*^{Col2ER} mice.

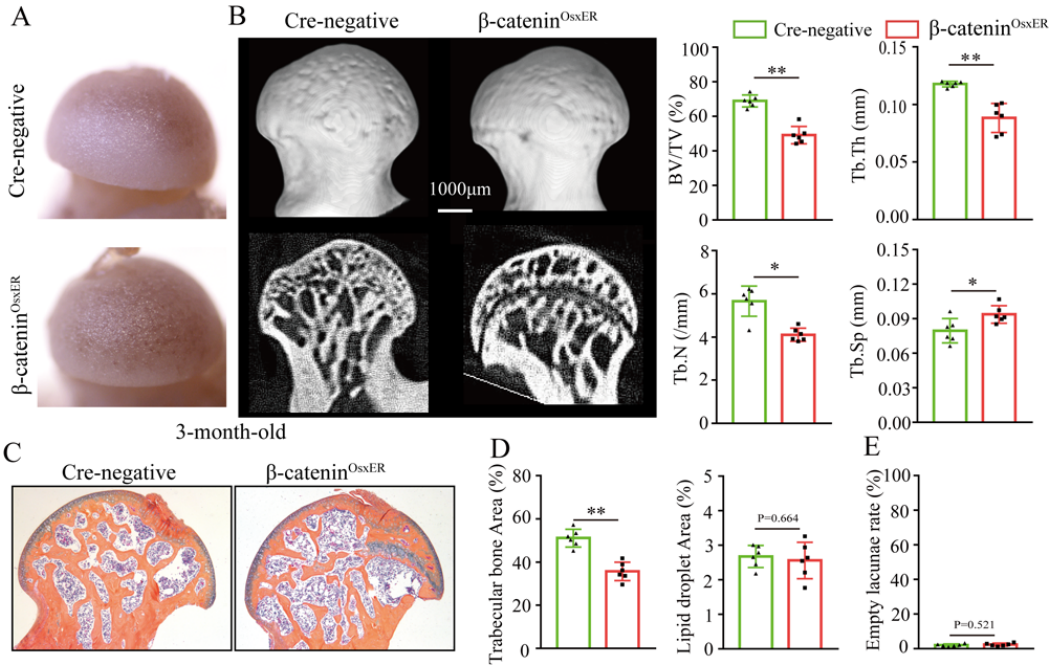

Figure 6. Loss-of-function of *β-catenin* in Osx^{+} cells causes bone loss in the femoral head. Femoral heads were harvested from 3-month-old *β-catenin*^{OsxER} mice and *Cre*-negative littermates with 5 continuous dosage of TM injections (1 mg/10 g body weight) at the age of 2 weeks. (A) Gross anatomy analysis of femoral heads in *β-catenin*^{OsxER} mice and *Cre*-negative littermates. (B) μCT images and quantitative analysis of BV/TV, Tb. N, Tb. Th and Tb. Sp in the femoral heads of *β-catenin*^{OsxER} mice. (C) ABH staining of femoral heads in *β-catenin*^{OsxER} mice. (D) Histomorphological quantitative analysis of trabecular bone area and fat droplet area in the femoral heads of *β-catenin*^{OsxER} mice. (E) Histomorphological quantitative analysis of empty lacunae rate in the femoral heads of *β-catenin*^{OsxER} mice.

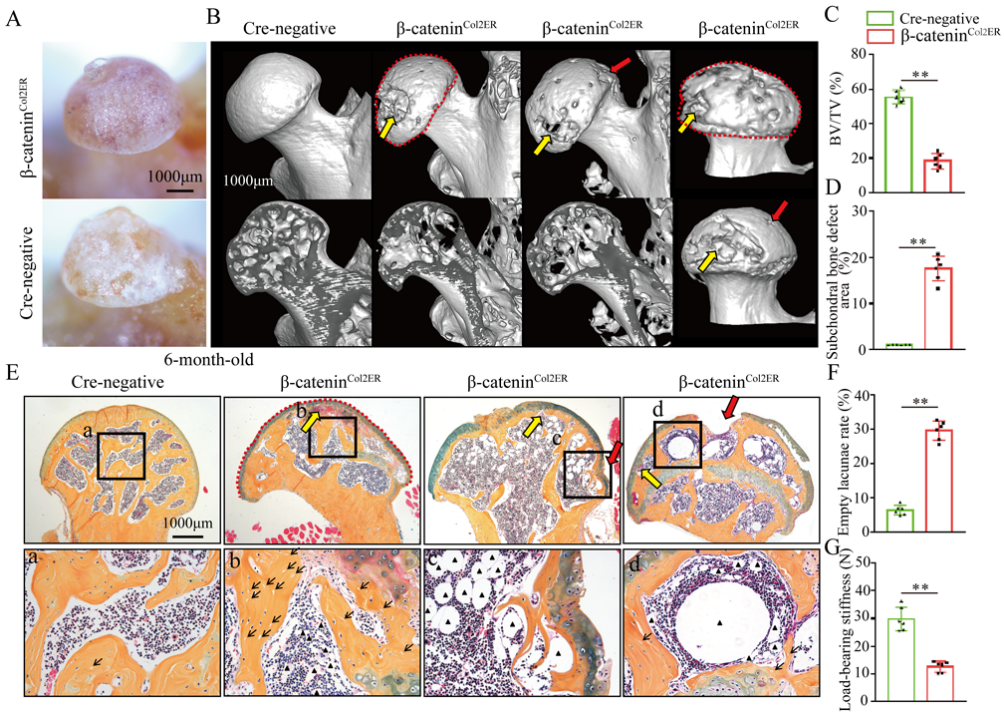

Figure 7. Older *β-catenin*^{Col2ER} mice display subchondral bone destruction and collapse tendency in femoral heads. Femoral heads were harvested from 6-month-old *β-catenin*^{Col2ER} mice and *Cre*-negative littermates with 5 continuous dosage of TM injections (1 mg/10 g body weight) at the age of 2 weeks. (A) Gross anatomy analysis of femoral heads in 6-month-old *β-catenin*^{Col2ER} mice. (B) Representative μCT images of femoral heads in 6-month-old *β-catenin*^{Col2ER} mice. Red dotted lines: integral deformity. Red arrows: local collapse. Yellow arrows: subchondral bone destruction. (C) Quantitative analysis of BV/TV in the femoral heads in 6-month-old *β-catenin*^{Col2ER} mice. (D) Quantitative analysis of subchondral bone defect area on the femoral head surface in older *β-catenin*^{Col2ER} mice. (E) ABH staining of femoral heads in 6-month-old *β-catenin*^{Col2ER} mice. a-c: high magnification images of representative subchondral bone region. Red dotted lines: integral deformity. Red arrows: local collapse. Black arrows: empty lacunae of osteoctye. Black triangles: fat droplet. (F) Histomorphological quantitative analysis of empty lacunae rate. (G) Loading-bearing stiffness of the femoral heads in 6-month-old *β-catenin*^{Col2ER} mice.

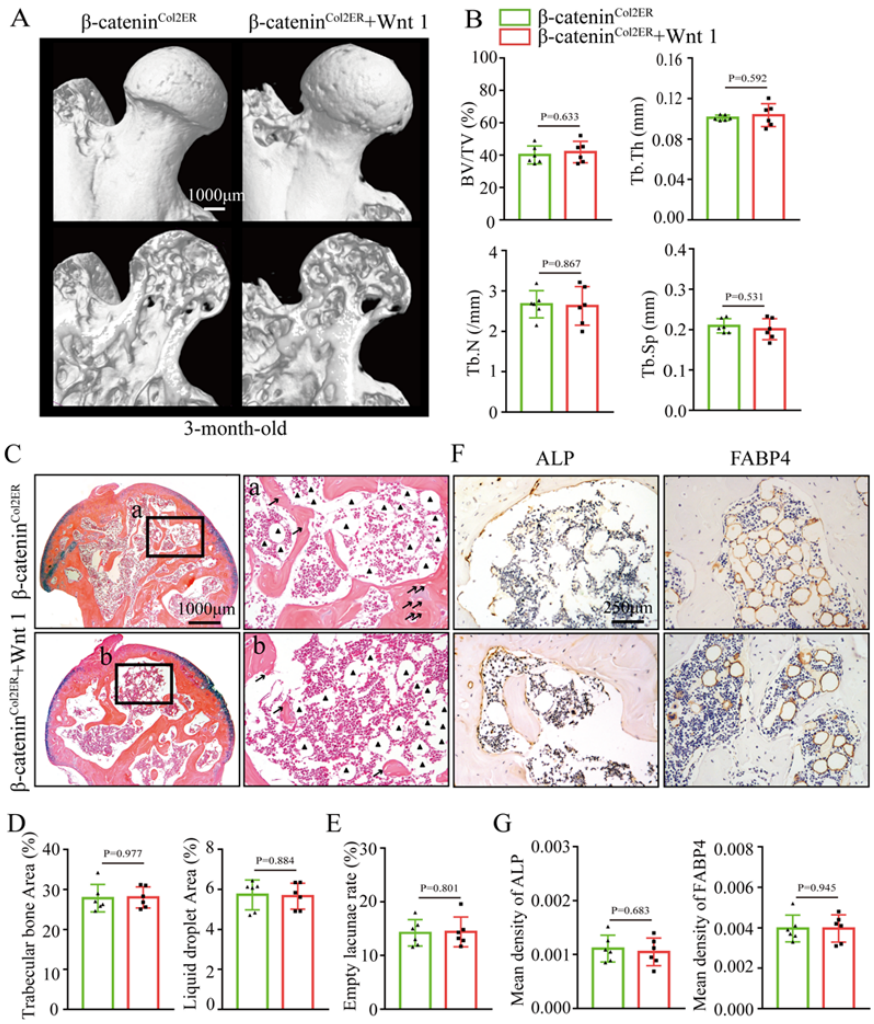

Figure 8. Systemic injection of Wnt agonist 1 can not alleviate the GONFH-like phenotype in *β-catenin*^{Col2ER} mice. *β-catenin*^{Col2ER} mice with 5 continuous dosage of TM injections (1 mg/10 g body weight) were treated with Wnt agonist 1 three times once week until sacrifice at the age of 3 months. (A) Representative μCT images of femoral heads in Wnt agonist 1 treated *β-catenin*^{Col2ER} mice. (B) Quantitative analysis of BV/TV, Tb.N, Tb.Th and Tb.Sp in the femoral heads of Wnt agonist 1 treated *β-catenin*^{Col2ER} mice. (C) ABH staining of the femoral heads in Wnt agonist 1 treated *β-catenin*^{Col2ER} mice. a-b: high magnification images of subchondral bone region. Black triangles: fat droplet. (D) Histomorphological quantitative analysis of trabecular bone area and fat droplet area in the femoral heads of Wnt agonist 1 treated *β-catenin*^{Col2ER} mice. (E) Histomorphological quantitative analysis of empty lacunae rate in the femoral heads of Wnt agonist 1 treated *β-catenin*^{Col2ER} mice. (F, G) IHC staining and quantitative analysis of ALP and FABP4 in the femoral heads of Wnt agonist 1 treated *β-catenin*^{Col2ER} mice.